Analyst

ROYAL SOCIETY OF CHEMISTRY

COMMUNICATION

View Article Online
View Journal | View Issue

Cite this: *Analyst*, 2020, **145**, 4124

Received 22nd April 2020,
Accepted 25th May 2020

DOI: 10.1039/d0an00809e

rsc.li/analyst

3D printed O_2 indicators†

Dilidaer Yusufu, Ri Han and Andrew Mills *

A polymer filament, containing an O_2-sensitive lumophore pigment, platinum(II) (pentafluorophenyl) porphyrin coated onto nanoparticulate silica particles, *i.e.* PtTFPP/SiO_2, is produced and used in a filament which is then 3D printed as O_2-sensitive indicator dots (1 cm diameter, 30 μm thick) on a polyethylene terephthalate (PET) supporting film substrate. Two different filaments, prepared using the polymers, low density polyethylene (LDPE) and polylactic acid (PLA), respectively, are used to produce 3D printed PtTFPP/SiO_2/LDPE and PtTFPP/SiO_2/PLA O_2-sensitive indicator dots, with dynamic ranges of 0–30% and 0–400% O_2, respectively. The O_2 response characteristics of these two, very different, indicator dots, such as sensitivity, response time and temperature sensitivity, are measured and compared with those of a commercial O_2 indicator, FOSPOR (OceanInsight) and other commercial O_2 indicators. The potential of this method for mass manufacture of O_2 indicator dots and the likelihood that it can be extended to produce other optical indicators, such as those for ammonia or CO_2, are discussed briefly.

The measurement of O_2 levels is important in a wide number of different fields, including chemical and clinical analysis, food packaging and environmental monitoring.[1–3] Conventional O_2 analysis usually involves common analytical techniques, such as gas chromatography or electrochemical analysis (*e.g.* using a Clark cell[4] for example), that are expensive and often lab-based as they require bulky instrumentation and/or technical support. As a result, in recent years there has been a growing interest in the development of novel optical indicators for the detection of O_2.[5] Most optical indicators for O_2 detection are based on the quenching of the luminescence of an electronically excited lumophoric dye, D*, by O_2,[5] *i.e.*

$$D^* + O_2 \xrightarrow{k_q} D + O_2^* \quad (1)$$

where D is the electronic ground state of the dye and k_q is the bimolecular quenching rate constant, which is often diffusion-controlled.[3] In a homogeneous microenvironment, usually the luminescent intensity, I, or lifetime, τ, exhibited by the dye is related to the concentration of O_2, $[O_2]$, *via* the Stern–Volmer equation,[6] *i.e.*

$$I_0/I = \tau/\tau_0 = 1 + K_{sv}[O_2] = 1 + k_q\tau_0[O_2] \quad (2)$$

where I_0 and I (or, τ_0 and τ) are the steady-state luminescence intensities (or, lifetimes) in the absence and presence of the O_2, respectively, and K_{sv} is the Stern–Volmer quenching constant. The concentration of O_2 is usually reported in units of $\%O_2$, where $\%O_2 = 100 \times P_{O_2}$, and P_{O_2} is the partial pressure of O_2 in the ambient environment, with units of atm. As a consequence, eqn (2) can be rewritten as

$$I_0/I = \tau/\tau_0 = 1 + K_{sv}'\%O_2 \quad (3)$$

where $K_{sv}' = \tau_0 k_q S_{O_2}$, and where S_{O_2} is the solubility coefficient of O_2 in the encapsulation medium. The value of $1/K_{sv}'$, usually referred to as $PO_2(S = 1/2)$,[7–9] provides an easy and rough measure of the sensitivity of the O_2 indicator since it is the level of oxygen required to produce a 50% reduction in I_0, or τ_0.

Most commercial optical indicators for O_2 are based on the luminescence quenching reaction (1), with quenching by O_2 described by eqn (3), in which they often use a very lipophilic lumophore such as platinum(II) (pentafluorophenyl) porphyrin, PtTFPP, or Pt(II) tetrabenzoporphyrin, PtTBP, embedded in a hydrophobic polymer. Some examples of such commercial O_2 indicators and their performance characteristics and current cost are listed in Table 1.

As illustrated by the data in Table 1, a striking feature of all such commercial O_2 indicators is the high cost of the indicator, which is usually in the form of a label and is either self-adhesive or needs to be stuck on. As noted by others, this high cost is because of the complexity of manufacture which is 'slow and difficult to control and standardise'.[17]

School of Chemistry and Chemical Engineering, Queens University Belfast, David Keir Building, Stranmillis Road, Belfast, BT95AG, UK.
E-mail: andrew.mills@qub.ac.uk

†Electronic supplementary information (ESI) available. See DOI: 10.1039/d0an00809e

Table 1 Features of some current commercial O_2 indicators[3]

Company	Product name	Operating range	Lower detection limits	Response time (s)	Lumophore	Price ($)	Ref.
Ocean insight	FOSPOR	0–100%	0.1%	<5	PtTFPP	36	10 and 11
PreSens	Pst3	0–100%	0.03%	<6	PtTFPP	33	12 and 13
Mocon	OpTechTM-O_2 platinum	0–30%	0.03%	<3	PtTBP	3	14 and 15
PyroScience	OXSP5	0–100%	0.02%	<7	PtTBP	33	16

As a consequence, although commonly used in many different areas, especially for research and product development, O_2 optical indicator technology has not found widespread use in applications, such as in packaging, where they are likely to have significant impact but which would require their low-cost mass manufacture and subsequent large-scale utilisation. Indeed, Kelly *et al.*, commenting on O_2 optical indicators, notes that in order 'to become viable in mass-scale packaging applications, indicator costs need to be reduced by at least ~2 orders'.[17]

In recent years, 3D printing has been utilised by many industries, such as aeronautics, industrial tooling, healthcare (pills and medical devices), construction, robotics, and the automotive industry, for the large scale production of 3D printed parts and products.[18] The advantages 3D printing has over most other methods of manufacture include speed of production of the final item, low initial capital investment cost, greater flexibility in product design and changing product design, less material waste and often a lower per item production cost, since it usually involves single step manufacture and near zero labour costs.[19,20] It is not surprising, therefore, to find that 3D printing is used increasingly in the manufacture of indicators,[21] but almost always to make a device, such as a micro-fluidic or electrochemical cell, which houses or utilises the key indicator chemical or biochemical elements, with the latter being added after the 3D printing process.[21] Reports of polymer filaments incorporated with sensor materials are mostly related to conductive applications, such as conductive polymers incorporated with carbon black, carbon nanotube or graphene.[22–24]

To our knowledge, there have been no previous reports of a 3D printed optical gas indicator produced by printing a filament containing the indicator. Thus, in this paper we report the first examples of a 3D printable, optical O_2 indicator-containing filament that is used to produce rapidly, easily and reproducibly O_2 indicator dots that have performance characteristics on a par with those of current commercial O_2 indicators, but that are likely to be produced at a fraction of the cost, due to the simplicity and scalability of their method of production.

In all this work the lumophore used was PtTFPP, from Inochem plc (Carnforth, UK), and the O_2-sensitive pigment was made by coating the PtTFPP on hydrophilic fumed silica particles (Aerosil 130 V (Evonik Industries, Essen, Germany), particle size ~20 nm). Briefly, 100 mg of PtTFPP were dissolved in the 100 mL acetone, after which 2 g of hydrophilic silica were added, the mixture stirred for 1 h and the acetone removed by rotary evaporation to leave a pink-coloured solid residue which was the 5 wt% PtTFPP/SiO_2 pigment. This O_2-sensitive lumophoric pigment was then used to make an O_2 indicator-containing filament by mixing 1 g of the pigment with 19 g of LDPE pellets (Ultrapolymers Warrington, UK) and feeding this mixture into a Rondol (Staffordshire, UK) Microlab twin-screw extruder, thermostatted at 90 °C at the feed zone and with a temperature profile which gradually increased along its length to 140 °C at the exit die zone. The extruder screw speed was always run at 80 rpm. The extruded product, a 2 mm diameter filament, was withdrawn at a rate of 0.9 m min^{-1} and chopped up, using an inline pelletiser, into 3 mm long pellets to create the PtTFPP/SiO_2/LDPE indicator masterbatch. The pellets of this masterbatch were then fed through the extruder 3 more times to ensure a homogeneous distribution of the pigment throughout each pellet. These fully-mixed, masterbatch pellets were then fed through the extruder one last time, but with an adjusted filament pulling speed so as to generate a 5 wt% (PtTFPP/SiO_2) pigmented LDPE filament, *i.e.* PtTFPP/SiO_2/LDPE filament, with a diameter of 1.75 ± 0.05 mm, as required for the 3D printer. A 3D printable 5 wt% (PtTFPP/SiO_2) pigmented PLA filament, *i.e.* a PtTFPP/SiO_2/PLA filament, was also produced using the same experimental procedure as above, but with an extruder temperature gradient of 100 to 180 °C.

The O_2 indicator-loaded filament was then 3D printed as a 1.0 cm diameter, 30 μm thick, indicator dot on a 50 μm thick PET sheet supporting substrate placed on the glass platform of the printer heated to 80 °C (LDPE indicator) or 60 °C (PLA indicator). The 3D printer used was a ZMorph[25] (Wroclaw, Poland) VX Full Set FDM, fitted with 0.3 mm nozzle and the LDPE indicator dots were printed at 135 °C, whereas the PLA printed dots were printed at 200 °C. Fig. 1 illustrates digital images of a typical, 3D printed PtTFPP/SiO_2/LDPE indicator

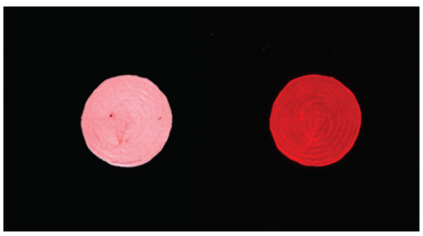

Fig. 1 Photographs of a 30 μm thick 3D printed PtTFPP/SiO_2/LDPE indicator dot with 1 cm diameter taken under daylight in air (left), and under UV light in an Ar atmosphere (right).

dot in air under daylight illumination and in Ar under UV illumination, provided by a 365 nm LED, 2 mW cm^{-2}, thereby revealing its pink colour, λ(max) absorption 390, 506, 539 nm, and luminescent nature (λ(max) emission 642 nm), respectively. The adhesion of both the 3D printed LDPE and PLA indicator dots to the PET supporting substrate was sufficient to pass the 3 M Scotch™ Tape Adhesion test (ASTM D3359-017).[26]

Further details regarding the absorption and emission peaks exhibited by PtTFPP in solution,[27] LDPE, PLA and polystyrene (PS)[28] are given in section S1 in the Electronic Supplementary Information, *i.e.* ESI.† A comparison of this spectroscopic data for PtTFPP in solution, to that of PtTFPP embedded in the different polymers reveals very little difference in the values of λ_{max} (absorption). The same striking similarity in λ_{max} values is found for the emission spectrum of the dye, although in solution the main emission band at 647 nm has an additional shoulder band at 705 nm,[27] which is absent when the dye in embedded in LDPE, PLA or PS.

A brief inspection of the daylight illuminated image of a typical O_2 dot illustrated in Fig. 1 reveals it to have a reasonably uniform colour but with one or two flecks of dark red. These same features are also seen (although as white flecks) when the same dots are printed using non-pigmented LDPE and PLA and are due to imperfect printing. This feature is not too surprising given that the 3D printer was used to deposit films that are thinner (30 μm) than its specifications suggest is possible (50 μm).[25] Smoother films will be produced if a higher specification 3D printer is used.

The 50 μm thick PET polymer supporting film substrate was chosen as this polymer is commonly used in food packaging, and so its use demonstrates that 3D printing could be used to print the indicator dot directly onto the packaging itself, if required. However, the supporting substrate is not limited just to PET, and other work showed that almost any polymer film could be used in its place, such as polypropylene, polyvinyl acetate and polystyrene, as well as ceramics, such as glass, and flexibles, such as paper and fabrics.

As indicated by eqn (3), it is possible to probe the sensitivity of any luminescence-based O_2 indicator by monitoring either its luminescence intensity, I, or lifetime, as a function of $\%O_2$ and in this work we monitored I, using a PerkinElmer LS 45 Fluorescence Spectrometer, with an excitation wavelength of 390 nm.

In a typical experiment, an O_2-sensitive dot on PET film was placed inside a plastic fluorescence cell, along the latter's diagonal, so that it made an angle of 45° to the excitation beam of the fluorimeter, which allowed its luminescence to be easily monitored. O_2/Ar gas mixtures of known composition, *i.e.* known $\%O_2$ level, produced using a gas blender, were flowed into the cell and the emission spectrum of the dot recorded after 5 min gas purging with each different O_2/Ar mix.

A typical set of emission spectra, recorded for the 3D printed PtTFPP/SiO_2/LDPE O_2 indicator dot, when exposed to a wide range of different O_2/Ar gas mixtures at 18 °C, is illustrated in Fig. 2. As illustrated by the insert plot in Fig. 2, a

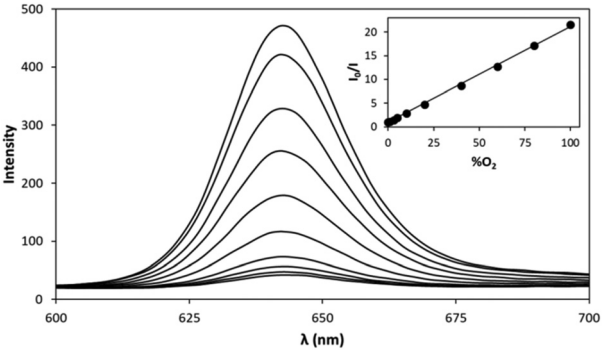

Fig. 2 Emission spectra of 3D printed PtTFPP/SiO_2/LDPE indicator dot upon exposure to (from top to bottom): 0, 1, 3, 5, 10, 20, 40, 60, 80, 100% O_2. Inset is a Stern–Volmer plot of the intensity data at 642 nm, illustrated in the main diagram, which a K_{sv}' value of (0.205 ± 0.002) % O_2^{-1} and a $PO_2(S = 1/2)$ value of 4.88%O_2.

Stern–Volmer plot of the intensity of luminescence at λ(max) emission (*i.e.* 642 nm) as a function of $\%O_2$ yielded a good straight line with a gradient (*i.e.* K_{sv}' value) equal to (0.205 ± 0.002) $\%O_2^{-1}$ and so a $PO_2(S = 1/2)$ value for the PtTFPP/SiO_2/LDPE indicator dot of *ca.* 4.88%O_2.

For comparison purposes, a similar set of experiments as those described above were conducted using a commercial OceanInsight FOSPOR O_2 indicator. This work yielded a similar set of results to those illustrated in Fig. 2, and a linear Stern–Volmer plot with a gradient of (0.0586 ± 0.0007) $\%O_2^{-1}$, *i.e.* a $PO_2(S = 1/2)$ value of 17.1%O_2; see section S2, in the ESI.† Interestingly, the operating range of this indicator is reported by the manufacturer as 0–100%O_2 (see Table 1), but, at a $\%O_2$ value of 100% it can be shown that the value of I_0/I for the FOSPOR dot would be *ca.* 7. Following this guide as to how to estimate the maximum $\%O_2$ that defines the operating range of a typical commercial O_2 indicator, *i.e.* when I_0/I is *ca.* 7, it follows that the operating range of the PtTFPP/SiO_2/LDPE indicator dot is 0–30%O_2, *i.e. ca.* 3 times less than that of the FOSPOR dot.

From an initial consideration of the above results, it might not appear obvious why the PtTFPP/SiO_2/LDPE indicator dot and the FOSPOR O_2 indicator should be so very different in terms of O_2 sensitivity, with K_{sv}' values of 0.205 and 0.0586% O_2^{-1}, respectively, when both indicators utilise the same lumophore, namely, PtTFPP, see Table 1. However, a brief inspection of eqn (3) reveals that $K_{sv}' = 1/PO_2(S = 1/2)$, depends upon τ_0, k_q and S_{O_2}, and while the value of τ_0 will be largely independent of the polymer encapsulation medium, the values of k_q and S_{O_2} will not, since k_q depends upon the diffusion coefficient, D_{O_2}; and so both D_{O_2} and S_{O_2} depend upon the encapsulation polymer. This situation is simplified somewhat in that the product of these two parameters, D_{O_2} and S_{O_2}, is equal to the permeability of O_2 in the encapsulation polymer, P_m. Thus, the difference in O_2 sensitivity exhibited by the PtTFPP/SiO_2/LDPE and FOSPOR O_2 indicators is due to the difference in the values of P_m for the two different encapsulation polymers. An excellent review[29] describing in more detail the effect of

polymer permeability on the sensitivity of O_2 sensors has been reported previously. Unfortunately, the identity of the encapsulation polymer used in the FOSPOR O_2 indicator is not known, so all that can be said about the latter polymer is that it is likely to have a lower O_2 permeability than that of LDPE (P_m = 22×10^{-18} m^3 m m^{-1} s^{-1} Pa^{-1}).[30]

A more striking demonstration of the effect of P_m on O_2-indicator sensitivity, is provided by a comparison of the O_2 sensitivity of the PtTFPP/SiO_2/LDPE indicator dot, illustrated in Fig. 2, with that of the PtTFPP/SiO_2/PLA indicator dot, measured under identical conditions and illustrated in Fig. 3. A quick comparison of these two data sets, *i.e.* Fig. 2 and 3, reveals that the latter O_2 indicator is much less sensitive than the former, which is not surprising given the O_2 permeability of PLA is over 11.3 times less than that of LDPE, with $P_m = 1.94 \times 10^{-18}$ m^3 m m^{-1} s^{-1} Pa^{-1}.[30] As illustrated by the insert plot in Fig. 3, a Stern–Volmer plot of the intensity of luminescence at λ(max) emission (*i.e.* 645 nm) as a function of $\%O_2$, for the PtTFPP/SiO_2/PLA indicator dot, yielded a good straight line, which had a gradient (*i.e.* K_{sv}' value) equal to (0.0142 ± 0.0003) $\%O_2^{-1}$ and so a $PO_2(S = 1/2)$ value of 70.4%O_2. The latter value shows that the PtTFPP/SiO_2/PLA indicator dot is *ca.* 14.4 *x*'s less sensitive than that of the PtTFPP/SiO_2/LDPE indicator dot. Not surprisingly, this factor of 14.4 is very similar to the ratio of the O_2 permeabilities of PLA and LDPE (*i.e.* 11.3), which in turn is consistent with the importance P_m plays in deciding the efficacy of the quenching reaction (1), *via* eqn (3), and, therefore, the sensitivity of such O_2 indicators. Once again, assuming that the maximum $\%O_2$ that defines the operating range of an O_2 indicator is when I_0/I = *ca.* 7, the operating range of the PtTFPP/SiO_2/LDPE indicator dot is estimated to be 0–400%O_2, *via* extrapolation of the Stern–Volmer plot in Fig. 3.

Another important characteristic of any optical O_2 indicator is how rapidly it responds to a sudden change in $\%O_2$, and some manufacturer-reported response time values are given in Table 1. In contrast to film sensitivity, the response time exhibited by a film usually depends upon the rate of diffusion of the O_2 into and out of the encapsulation medium, respectively, and so depends upon D_{O_2}.[7,31] In this work, each of the three O_2 indicators, *i.e.* PtTFPP/SiO_2/LDPE, PtTFPP/SiO_2/PLA and FOSPOR, were exposed to an alternating cycle of Ar and 100% O_2 and the concomitant variation of the intensity of luminescence at λ(max) emission, *I*, recorded as a function of time, *t*; the results of this work are illustrated in S3 in the ESI.† An analysis of these results reveals values for their 90% response (*i.e.* Ar to O_2, luminescence decreases) times, *i.e.* $t_{\downarrow 90}$ values of 3, 41 and 3 s, respectively. The ratio of the $t_{\downarrow 90}$ values for the PtTFPP/SiO_2/PLA and PtTFPP/SiO_2/LDPE indicators, is equal to 13.7, and so, as might be expected, similar to that of the O_2 permeabilities of PLA and LDPE (*i.e.* 11.3), given that D_{O_2} varies much more than S_{O_2} for most polymers.[32]

As indicated by the response and recovery profiles illustrated in S3 in the ESI,† the degree of drift exhibited by all three O_2 indicators is very small and similar, both in O_2 and Ar. This is perhaps not too surprising given they all use the same lumophore, which is noted for its photostability.[28,29] For reference, OceanInsight report the drifts of the FOSPOR indicator as 0.0002% and 0.015% in Ar and pure O_2, respectively,[33] and there appears no obvious reason why the 3D printed O_2 dots shouldn't exhibit similar drift values.

As noted above most, if not all, O_2 optical indicators exhibit a sensitivity, a measure of which is $PO_2(S = 1/2)$ or K_{sv}', that depends on the O_2 permeability of the encapsulation polymer, *i.e.* P_m. As noted earlier, P_m is the product of D_{O_2} and S_{O_2}, both of which are temperature-sensitive parameters, with D_{O_2} increasing, and S_{O_2} decreasing, with increasing temperature. It follows that the sensitivity of all such O_2 optical indicators varies with temperature, usually increasing with increasing temperature, which suggests that the positive activation energy value associated with D_{O_2}, is bigger than the negative activation energy value associated with S_{O_2} for most encapsulation polymers.

Clearly, temperature sensitivity is an important characteristic of any O_2 indicator and so was measured for each of the PtTFPP/SiO_2/LDPE, PtTFPP/SiO_2/PLA and FOSPOR O_2 indicators by recording the variation of *I* as a function of $\%O_2$, at a series of different temperatures spanning the range 5–35 °C. The Stern–Volmer plots arising from this data generated a range of values of K_{sv}' as a function of temperature, *T*. An Arrhenius plot of this data, *i.e.* $\ln(K_{sv}')$ *vs.* *T*, for each of the O_2 indicators, illustrated in S4 in the ESI,† yielded a good straight line, from the gradient of which a value of the activation energy, $-\Delta H$, associated with K_{sv}' was calculated. For the PtTFPP/SiO_2/LDPE, PtTFPP/SiO_2/PLA and FOSPOR O_2 indicators the following values of $-\Delta H$ were determined 23.3, 16.5 and 13.1 kJ mol^{-1}, respectively, a brief inspection of which reveals that the two 3D printed indicators are slightly more temperature sensitive than the commercial FOSPOR indicator. Using the above values for $-\Delta H$ it can be shown that at 18 °C, the temperature sensitivities of the PtTFPP/SiO_2/LDPE, PtTFPP/SiO_2/PLA and FOSPOR O_2 indicators, as measured by K_{sv}', when expressed as a percentage of K_{sv}', *i.e.* $\%K_{sv}'/°C$ (see Table 2 for definition), are 3.2, 2.3 and 1.9% per °C, respect-

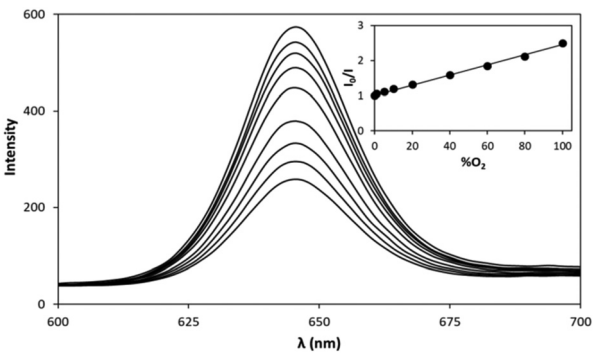

Fig. 3 Emission spectra of 3D printed PtTFPP/SiO_2/PLA indicator dot upon exposure to (from top to bottom): 0, 1, 3, 5, 10, 20, 40, 60, 80, 100% O_2. Inset is a Stern–Volmer plot of the intensity data at 645 nm, illustrated in the main diagram, which a K_{sv}' value of (0.0142 ± 0.0003) $\%O_2^{-1}$ and a $PO_2(S = 1/2)$ value of 70.4%O_2.

Table 2 O_2 sensitive characteristics of the 3D printed O_2 indicators and the FOSPOR indicator

Indicators	3D printed PtTFPP-LDPE dot	3D printed PtTFPP-PLA dot	FOSPOR
Operating range[a]	0–30%	0–400%	0–100%
Lower detection limits	0.05%	0.1%	0.1%
K_{sv} ($\%O_2^{-1}$)	0.205 ± 0.002	0.0142 ± 0.0003	0.0586 ± 0.0007
$PO_2(S = 1/2)$ ($\%O_2$)	4.88	70.4	17.1
t_{190} (s)	3	41	3
ΔH (kJ mol^{-1})	23.3	16.5	13.1
$\%K_{sv}'/°C$[b]	3.2%	2.3%	1.9%
Price ($)	0.007[c]	0.009[c]	36

[a] Top range value based on $\%O_2$ when $I_0/I = 7$. [b] $\%K_{sv}'/°C = 100x(dK_{sv}'/dT)/K_{sv}'$ at 18 °C. [c] Calculated based on cost of chemicals.

ively. Because most optical O_2 indicators, including the ones reported here, are temperature sensitive, all work with such indicators requires knowledge of the temperature of the system, and this is usually provided by using a contact thermocouple-based temperature probe or contactless IR temperature probe.[1] Knowledge of the temperature allows these probes to operate typically over the temperature range 0–50 °C.[1]

Although all of the above work was carried out using dry gas mixtures, other work, using the wet (*i.e.* 100% relative humidity) equivalent gas mixtures, showed no change in the performance characteristics of the PtTFPP/SiO_2/LDPE, PtTFPP/SiO_2/PLA and FOSPOR O_2 indicators, a summary of which is given Table 2.

As noted earlier, the major problem with most commercial optical O_2 indicators is the complex nature of their production which results in a high cost, typically $3-36 per indicator, see Table 1.[3] This high cost has proved a major barrier to their routine and widespread use in food packaging for example.[3] Calculations of the cost of the two different 1 cm diameter 3D printed O_2-sensitive dots reported in this work were made based on the cost of chemicals used and, in both cases, was found to be <1 cent, see Table 2. Note, this cost would obviously be much less if a smaller dot was printed as is likely to be the case; for example, indicator dots with diameters of 0.5 cm or 0.25 cm would be 4 or 16 *x*'s less expensive (in terms of chemical costs) than a 1 cm diameter dot. Obviously, the low chemical costs of the indicator dots given in Table 2 cannot be taken as a measure of their eventual retail cost. However, this feature and, more importantly, the simplicity and scalability of the method by which they are produced makes it likely that they will retail at a much lower price than their current commercial counterparts which, as others have noted, are 'difficult to manufacture'.[17]

Other work carried out on the 3D printed O_2 sensitive dots showed that large batches, *i.e.* arrays, can be easily printed on one sheet of PET and that the reproducibility of such batches, in terms of O_2 sensitivity, within a batch (typically containing 9 indicator dots) and from batch to batch was >98.5%.

In conclusion, PtTFPP/SiO_2/LDPE and PtTFPP/SiO_2/PLA O_2-sensitive indicator dots can be 3D printed from an appropriate O_2-sensitive lumophore-containing filament prepared by extrusion. Since both polymer extrusion and 3D printing are common, relatively inexpensive, scalable processes, this method provides a route for the mass production of inexpensive O_2 indicators. There also appears no reason why other optical indicators, such as those for ammonia,[34] and CO_2[35] cannot be produced in the same way. Thus, this work represents the first of a possible wide range of optical indicators that could be produced by 3D printing, which would in turn provide a route to their inexpensive mass manufacture and subsequent widespread utilisation in such diverse areas as: packaging, clinical analysis and environmental monitoring.

Conflicts of interest

There are no conflicts to declare.

Notes and references

1 A. Mills, *Chem. Soc. Rev.*, 2005, **34**, 1003–1011.
2 X.-D. Wang and O. S. Wolfbeis, *Anal. Chem.*, 2013, **85**, 487–508.
3 S. Banerjee, C. Kelly, J. P. Kerry and D. B. Papkovsky, *Trends Food Sci. Tech.*, 2016, **50**, 85–102.
4 L. C. Clark Jr., R. Wolf, D. Granger and Z. Taylor, *J. Appl. Physiol.*, 1953, **6**, 189–193.
5 X.-D. Wang and O. S. Wolfbeis, *Chem. Soc. Rev.*, 2014, **43**, 3666–3761.
6 J. Lakowicz, *Principles of Fluorescence Spectroscopy*, Kluwer-Plenum, New York, USA, 2nd edn, 1999.
7 A. Mills and A. Lepre, *Anal. Chem.*, 1997, **69**, 4653–4659.
8 A. Mills, *Platinum Met. Rev.*, 1997, **41**, 115–127.
9 A. Mills and A. Graham, *Analyst*, 2013, **138**, 6488–6493.
10 OceanInsight, https://www.oceaninsight.com/support/calibration-services/oxygen-sensor-calibration/, accessed May 2020.
11 M. R. Shahriari, *US Pat*, 20080199360A1, 2007.
12 PreSens, https://www.presens.de/products/detail/oxygen-sensor-spot-sp-pst3-nau, accessed May 2020.
13 I. Klimant, *US Pat*, 6770220B1, 1999.
14 Mocon, https://www.ametekmocon.com/products/headspacemapgasanalyzers/optech, accessed May 2020.
15 D. W. Mayer, *EU Pat*, 2455746B1, 2010.
16 PyroScience, https://www.pyroscience.com/en/products/all-sensors/oxsp5#Compatible-meters, accessed May 2020.

17 C. Kelly, D. Yusufu, I. Okkelman, S. Banerjee, J. P. Kerry, A. Mills and D. B. Papkovsky, *Sens. Actuators, B*, 2020, **304**, 127357, DOI: 10.1016/j.snb.2019.127357.
18 R. Horne and K. Hausman, *3D Printing For Dummies*, John Wiley & Sons, Inc., Hoboken, NJ, USA, 2nd edn, 2017, pp. 33–49.
19 B. Redwood, F. Schoffer and B. Garret, *The 3D Printing Handbook: Technologies, Design and Applications*, 3D Hubs B.V., Amsterdam, The Netherlands, 2018, 241–279.
20 B. Berman, *Bus. Horiz.*, 2012, **55**, 155–162.
21 T. Han, S. Kundu, A. Nag and Y. Xu, *Sensors*, 2019, **19**, 1706, DOI: 10.3390/s19071706.
22 S. J. Leigh, R. J. Bradley, C. P. Purssell, D. R. Billson and D. A. Hutchins, *PLoS One*, 2012, **7**, e49365, DOI: 10.1371/journal.pone.0049365.
23 J. F. Christ, N. Aliheidari, A. Ameli and P. Pötschke, *Mater. Des.*, 2017, **131**, 394–401.
24 S. Krachunov and A. J. Casson, *Sensors*, 2016, **16**, 1635, DOI: 10.3390/s16101635.
25 ZMorph, https://www.zmorph3d.com, accessed May 2020.
26 Standard Test Methods for Rating Adhesion by Tape Test, ASTM D3359 – 17 https://www.astm.org/Standards/D3359.htm, accessed May 2020.
27 S.-W. Lai, Y.-J. Hou, C.-M. Che, H.-L. Pang, K.-Y. Wong, C. K. Chang and N. Zhu, *Inorg. Chem.*, 2004, **43**, 3724–3732.
28 S. K. Lee and I. Okura, *Anal. Commun.*, 1997, **34**, 185–188.
29 Y. Amao, *Microchim. Acta*, 2003, **143**, 1–12.
30 G. Colomines, V. Ducruet, C. Courgneau, A. Guinault and S. Domenek, *Polym. Int.*, 2010, **59**, 818–826.
31 A. Mills and Q. Chang, *Analyst*, 1992, **117**, 1461–1466.
32 K. Yam, *The Wiley Encyclopedia of Packaging Technology*, John Wiley and Sons, Inc., New York, USA, 3rd edn, 2009, pp. 551–555.
33 Optical sensor catalogue, http://www.oemoptic.ru/docs/cat/catalogsensors.pdf, accessed May 2020.
34 N. Wells, D. Yusufu and A. Mills, *Talanta*, 2019, **194**, 830–836.
35 A. Mills, in *Indicators and Environment, Health and Security*, ed. M. I. Baraton, Springer Science, Dordrecht, Netherlands, 2009, pp. 347–370.